



Article

## Effect of ethanol on the structure and aggregation properties of C<sub>60</sub> fullerenes

 Hakan Ozbay

Department of Physics, Faculty of Science, Erciyes University, Kayseri, Turkey

\*Correspondence: [hakan.ozbay@tutamail.com](mailto:hakan.ozbay@tutamail.com)

**Abstract.** This study investigated the effect of ethanol on the structure and aggregation properties of C<sub>60</sub> fullerenes using an atomic force microscope. The fullerenes were dissolved in ethanol with different concentrations (0%, 10%, 25%, 50%, 100%) and deposited on silicon substrate for further analysis. The results showed that the size of molecular aggregates of fullerenes increased significantly with increasing ethanol concentration, starting from 15-20 nm in the absence of ethanol and reaching 80-100 nm at 100% ethanol. At the same time, the structure of the aggregates became more friable, indicating the solvent effect of ethanol. The interaction force measurements showed that the adhesion force of fullerenes to the substrate decreased with increasing ethanol concentration, indicating a weakening of adhesion and molecular interactions. These data confirm the significant effect of ethanol on the physicochemical properties of fullerenes and can be used to develop nanomaterials with variable structural characteristics.

**Keywords:** Fullerenes, ethanol, atomic force microscope, aggregation, molecular interactions.

### 1. Introduction

Fullerenes are carbon molecules consisting of 60, 70, or more carbon atoms combined into a spherical, ellipsoidal, or tubular structure. The discovery of fullerenes, which resulted from the previous work, led to a significant increase in research in chemistry, physics, and materials science [1]. The discovery of new properties of fullerenes, such as their high chemical stability and unique optical, electrical, and mechanical characteristics, opened new horizons for the development of innovative technologies in a wide variety of fields.

The authors reported the discovery of the molecule C<sub>60</sub>, known as “buckyball”[2]. In the framework of experimental studies conducted with the help of laser evaporation of carbon in an inert gas, a set of molecules with a different number of carbon atoms was obtained, among which the main ones were C<sub>60</sub> and C<sub>70</sub>. Subsequently, their characteristic geometric structure was established - fullerene molecules are carbon networks that resemble soccer ball structures consisting of five- and hexagons.

One of the first directions of research was the study of structural and electronic properties of fullerenes. Studies of the molecular geometry of fullerenes showed that the molecule C<sub>60</sub> has the shape of an icosahedron consisting of 12 pentagons and 20 hexagons. This discovery was confirmed by X-ray diffraction and high-resolution microscopy, as well as by ab initio calculations based on quantum chemistry. Such structures provide unique mechanical and chemical properties of fullerenes that distinguish them from other carbon compounds. The study of the electrochemical properties of fullerenes has shown that they have an excellent ability to form ionized states, which is related to their electronic structure and features of transition states. Studies using spectroscopy have confirmed that fullerenes can function as electron acceptors, which makes them attractive for application in organic solar cells and other electronic devices [3], [4].

Fullerenes are highly chemically active, which opens up opportunities for the synthesis of various derivatives such as fullerene diols, amides, and salts. One of the popular methods for

modifying fullerenes is a reaction with various chemical agents, which allows them to change their physicochemical properties and use them as catalysts or in nanotechnology. For example, chemists have found that fullerenes can form strong bonds with various metals, such as gold and silver, which opens up opportunities for their use in catalysis [5]. In addition, fullerenes are being actively explored as molecules to create materials with improved mechanical and thermal conductive properties. One prominent example is the creation of composite materials based on fullerenes and carbon nanotubes, which can be used in electronics, sensors, and other devices [6].

In recent years, interest in studying the biological properties of fullerenes, including their biocompatibility and toxicity, has increased [7], [8]. Studies on the biological activity of fullerenes have shown that fullerenes can have antioxidant activity, which makes them promising for use in medicine. For example, fullerene C<sub>60</sub> has been proposed as an antioxidant that can neutralize free radicals and prevent oxidative stress in cells [9], [10].

Today, fullerenes are actively used in various fields, including electronics, photonics, and materials with improved mechanical and thermal properties, as well as in medicine and biotechnology. One of the most promising areas is the use of fullerenes in organic solar cells, where they can act as electron acceptors, improving the efficiency of photovoltaic cells [11]. Fullerenes also finds applications in the production of nanocomposites, and sensors, as well as in water purification and energy storage.

Despite the widespread use of fullerenes, their properties have not yet been fully disclosed. In connection with this task, this work reflects an attempt to reveal additional physical and mechanical properties of fullerenes. The work aims to determine the influence of different concentrations of ethanol on the aggregation properties of fullerenes, their interaction with the substrate, and structural changes at the molecular level.

## 2. Methods

The sample of fullerene C<sub>60</sub> was set to a large scanning range, between 10 and 80 μm. The height of the structures (more precisely, the depth of the depression) is approximately 1.6 μm. with the sample showing an ordered, repeating pattern (Figure 1). For the experiment, C<sub>60</sub> fullerenes were dissolved in ethanol with different concentrations (0%, 10%, 25%, 50%, 100%) and deposited on a silicon substrate. After the solution dried, the surface of the samples was examined by AFM in topographic scanning and interaction force mode. This equipment was manufactured by an american company TechSpin, Glass-based thin films with a thickness of less than 0.5 mm and a diameter of 120 nm were used as sample substrates, the surface of which was treated with ethanol solution. Epic Crystals company manufactured thin films. The treated sample was dried under ambient conditions at room temperature of 23 degrees Celsius, for 2 hours. Excessive moisture, dust, grease, or other surface contaminants are a few examples of contributing factors. Some samples therefore require particular processing in order to clean their surface. So, the sample was then placed in an oven at 250° for 2-3 hours. After complete cooling, the sample was placed in a microscope for visualization.

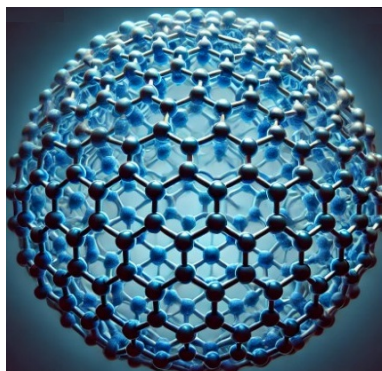


Figure 1 – Original structure of C<sub>60</sub>

The integral gain was set well below the optimum value. When the gain was reduced, the feedback loop was slow enough, as well as the elevation changes, to provide high resolution. Note the poorly defined edges in Figure 25, which were affected by the low gain. By gradually increasing the gain to values much higher than optimal, the Z-controller compensated for the feedback errors, which is called overshoot.

The atomic composition of the solid surface was studied using an atomic force microscope, which affects the behavior of the solid, these compositions are of great importance to the physics of materials (Figure 2).

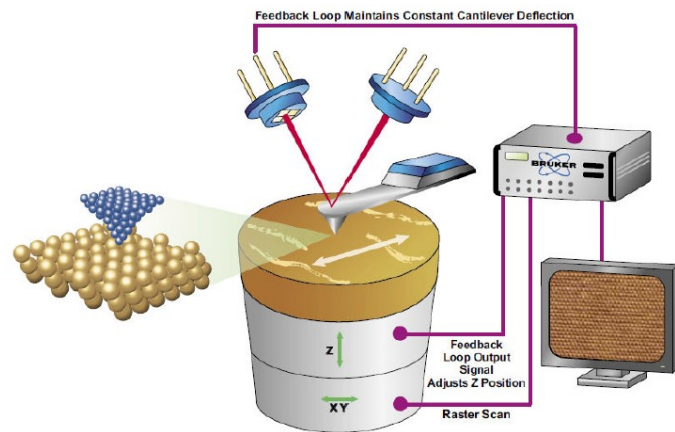


Figure 2 – The atomic force microscope configuration

The AFM measures the force interaction between a sample and a minuscule tip (less than 10 nm in radius) that is affixed to a cantilever, typically characterized by the Lennard-Jones potential. The interaction between the sample and the cantilever is derived from the superposition of the individual interactions. The cantilever's very end receives the concentrated laser beam and reflects it back to the segmented photodiode. As a result, the cantilever's angle of deflection increases; that is, a tiny offset of the cantilever causes a bigger offset of the reflected laser beam on the photodiode. The mechanical gain increases with distance from the diode. However, because of outside disturbances, the photodiode cannot be positioned too far away. The laser deflection method's sensitivity to light from the surrounding environment, light reflected from the sample or cantilever, and other potential light sources is one explanation for this. Deflections of less than one angstrom can be measured thanks to the optical detecting technology.

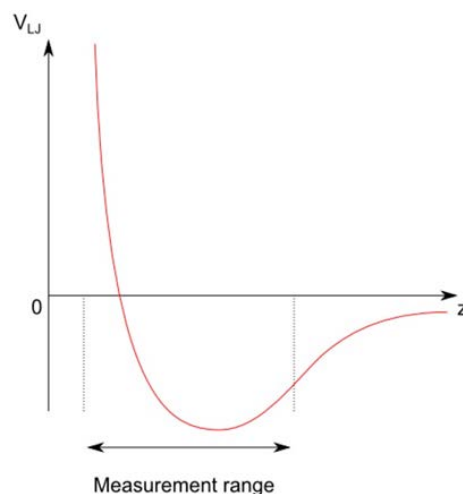


Figure 3 – The Lennard-Jones potential leads to attraction at long distances and repulsion at short distances

The schematic diagram of the feedback system is shown in Figure 4, which has the form of a PID controller. The feedback control system produces an AFM image where the cantilever deflection is deflected by a sensor. This position is then compared to a set point, i.e. a constant value of the cantilever deflection selected by the user. Since the cantilever deflection is directly related to the tip-sample interaction force. Typical force values are in the range of nN. The difference between the actual interaction force and the desired force is called the error signal. This error signal is used to move the tip or specimen to the distance at which the cantilever has the desired deflection. This displacement is plotted as a function of the lateral position of the tip and represents the so-called topography.

The goal of the feedback system is to quickly minimize the error so that the measured topography matches the real topography of the sample. Therefore, the error signal must be amplified by a PID (proportional-integral-differential) controller.

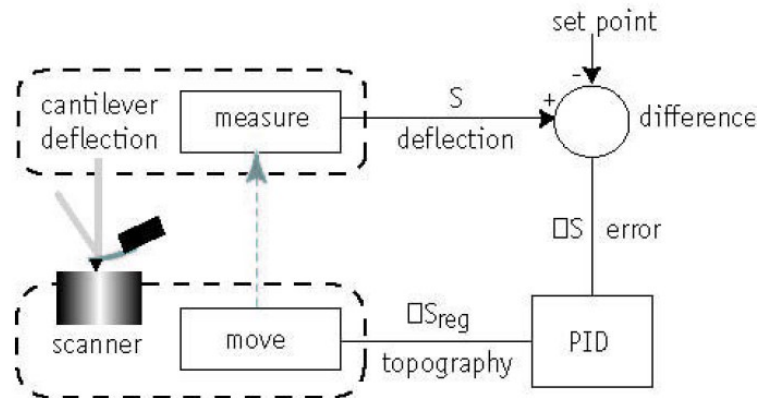


Figure 4 – The feedback system

The main task was to reproduce the rectangular tilt angle as accurately as possible. For this purpose, the gain of the PID controller was adjusted. Figure 5: P-Gain shows the result where only the proportional gain (P) was increased, where the relief shows the large rise time. (slope), overshoot (peak) and settling time (oscillation). Further, the differential gain (D) is increased in addition to P bl. Figure 6: PD-Gain shows that the derivative gain reduces both the overload, the settling time, and the rise time, but has virtually no effect on rise time. To see the effect of integral gain (I), we decreased the gain D while the gain I increased. The result of the calibration is shown in Figure 7, where the PI-Gain I control further reduced the overload and shortened the rise time.

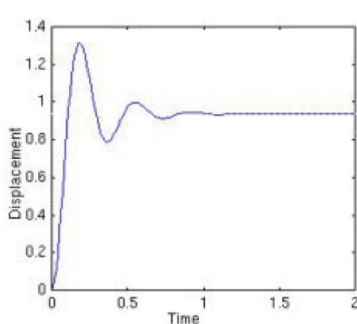


Figure 5 – P-Gain

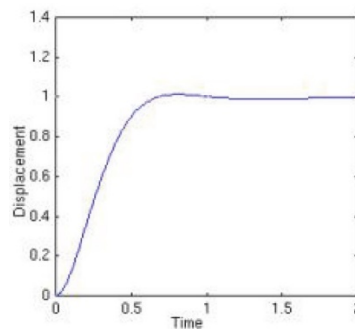


Figure 6 – PD-Gain

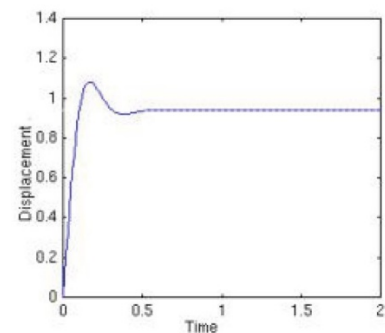


Figure 7 – PI-Gain

When probing the surface, the tip is always in touch with the sample. Thus, the user sets the cantilever's deflection and, consequently, the interaction force (set-point). The feedback regulator moves the scanner vertically toward the sample in order to preserve this setpoint. The sample's topography is then plotted using the movement that the regulation produces. The interaction force is the primary parameter to set in this mode. This needs to be set to a minimum such that the tip barely

touches the surface. This method's drawbacks include the possibility of sample and tip damage and the inability to properly photograph sticky samples.

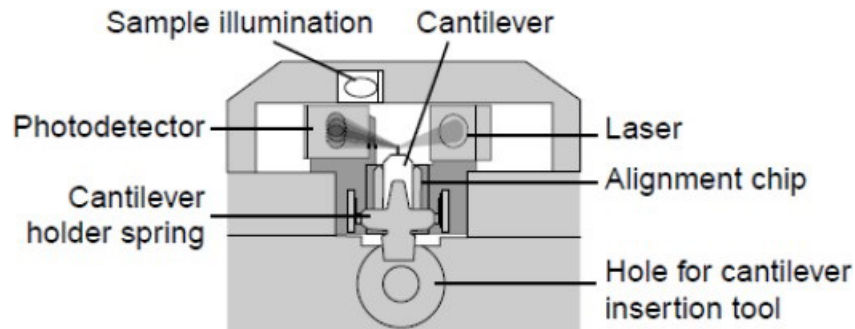


Figure 8 – Sample installation and calibration

Before starting the experiment, the instrument underwent a thorough calibration. At that, the cantilever tip was set at a distance of a fraction of a nanometer from the sample without touching it with excessive force. This delicate operation is performed in two steps: manual coarse approximation and automatic final approximation. The color of the indicator at the bottom of the software interface indicated the calibration status, where Orange/yellow indicated normal status during the approach, i.e., when the Z-scanner is fully extended toward the sample; red indicated that the approach had gone too far, i.e., the tip had entered the sample and the Z-scanner was fully extended away from the sample. Often this status indicates tip damage.

Correction of spectra in AFM scans was performed by taking into account several factors, including drive nonlinearity, temperature drifts, and topographic artifacts. The basic approach involves the use of calibration procedures and mathematical data processing. Firstly, the piezoelectric ACM actuator has a nonlinear response to the applied voltage. A dependence was applied to eliminate the distortion:

$$x_{real} = x_{rated} \cdot (1 + \alpha \cdot x_{rated}) \quad (1)$$

Where:  $x_{real}$  – corrected movement;  $x_{rated}$  – specified displacement;  $\alpha$  – nonlinearity coefficient. For spectral correction, background subtraction using a baseline approximation such as a polynomial was used:

$$I_{pure}(v) = I_{measured}(v) - P(v) \quad (2)$$

Where:  $I_{pure}(v)$  is the corrected signal;  $I_{measured}(v)$  is the original signal;  $P(v)$  is the baseline polynomial. These measures minimize systematic errors, improve the accuracy and reproducibility of the results, and ensure that the spectra can be correctly compared with experimental data from other methods.

### 3. Results and Discussion

By examining the ethanol-treated fullerene  $C_{60}$  using an AFM, the changes in its nanostructure can be studied in more detail. In its natural state, fullerene  $C_{60}$  has a characteristic molecular symmetry in which the carbon atoms form a strong spherical shell with alternating hexagons and pentagons. This stable framework accounts for the molecule's unique electronic and mechanical properties, including its high stability and ability to interact with other molecules such as solvents and various chemical reagents. When a fullerene interacts with ethanol, ethanol molecules adsorb on its surface. The ethanol molecules typically bind to the fullerene by weak intermolecular forces, including van der Waals interactions and hydrogen bonds, resulting in the formation of ethanol clusters on the surface of the fullerene. These clusters can take the form of discrete domains located across the surface of the fullerene sphere.

In AFM images of 10-15% ethanol-treated fullerene that is presented in Figure 9, such clusters appear as granular regions with increased height compared to smooth regions where ethanol

molecules are absent. The observed structural features depend on the processing parameters such as ethanol concentration, exposure time, temperature, and pressure. At low ethanol concentrations, single molecules or small clusters on the surface can be observed, whereas, at higher solvent concentrations, the fullerene is covered by a denser layer of ethanol molecules, resulting in a significant change in its surface morphology. Structural features observed on AFM include an increase in the local roughness of the fullerene surface and the appearance of microscopic bumps or “spots” that correspond to sites of ethanol adsorption. In some cases, with prolonged exposure, ethanol molecules can penetrate the intermolecular space of fullerenes in solid phases, leading to the formation of multilayer structures consisting of fullerenes and ethanol clusters.

Taking into account all of the above factors, atomic force microscopy reveals the following aspects of fullerene modification upon ethanol treatment. After ethanol treatment, inhomogeneous structures are formed on the surface of fullerene, which are visible as granular clusters or “spots”. The size and shape of these clusters depend on the treatment conditions.

Also, the presence of ethanol can affect the local electron density on the fullerene surface, leading to changes in the interactions with the AFM probe and the appearance of regions with different electronic contrasts.

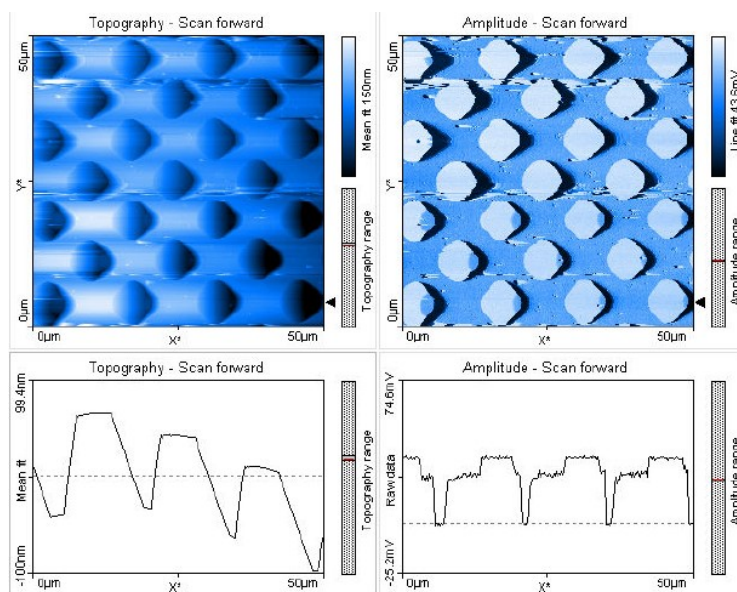


Figure 9 – The 10-15% ethanol-treated sample of C<sub>60</sub>

The interactions between fullerene and ethanol molecules occur mainly through weak forces such as hydrogen bonds and also due to  $\pi$ - $\pi$  interactions between aromatic carbon rings and ethanol molecules, which can lead to temporary fixation of ethanol molecules on the surface. As the temperature increases, some ethanol molecules may be desorbed and a transition to a more ordered state on the surface is observed. This emphasizes that the stability of the modified surface is temperature-dependent.

Topographic studies using AFM showed clear changes in the structure of fullerenes with increasing ethanol concentration. In the samples without ethanol (0%), fullerene molecules formed compact aggregations, the size of which did not exceed 15-20 nm. These structures had pronounced irregularities and negligible intermolecular gaps. However, when ethanol was added, the size of the aggregates began to increase. At 10% ethanol concentration, fullerene molecules formed larger clusters, the size of which varied from 30 to 35 nm. Despite the increase in the size of aggregates, the structure remained relatively compact.

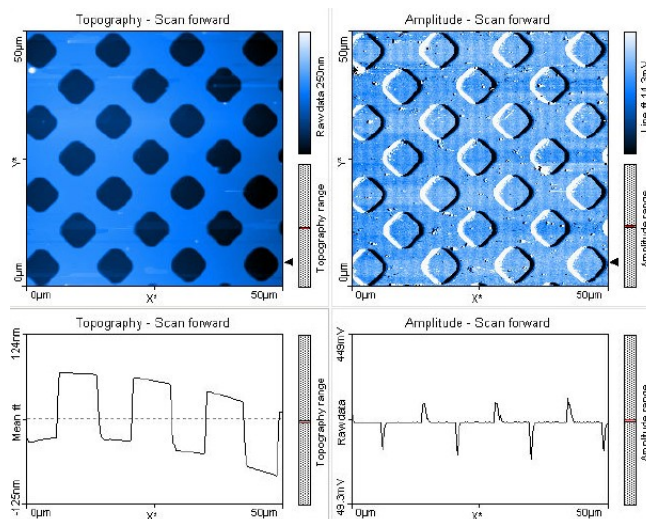


Figure 10 – The 25% ethanol-treated sample of  $C_{60}$

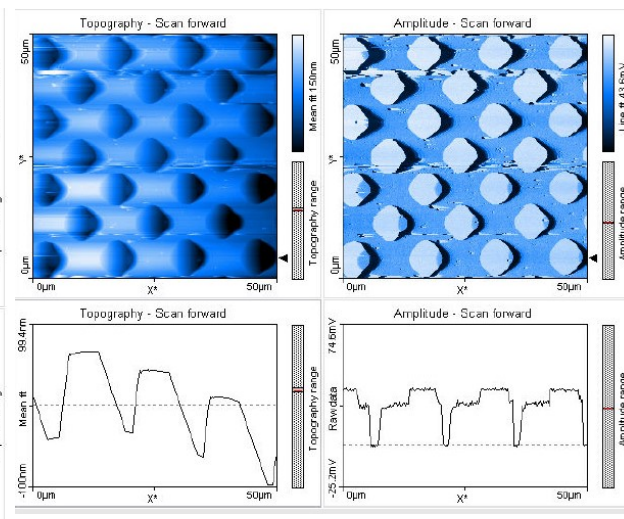


Figure 11 – The 50% ethanol-treated sample of  $C_{60}$

With increasing ethanol concentration (25% and higher), fullerenes began to form larger and looser aggregates. In samples with 25% ethanol, the size of clusters was 45-50 nm, and at 50% ethanol concentration, fullerenes formed structures of 60-65 nm. At 100% ethanol, fullerene molecules formed maximally large and loose aggregates with sizes up to 100 nm, with clearly pronounced gaps between molecules.

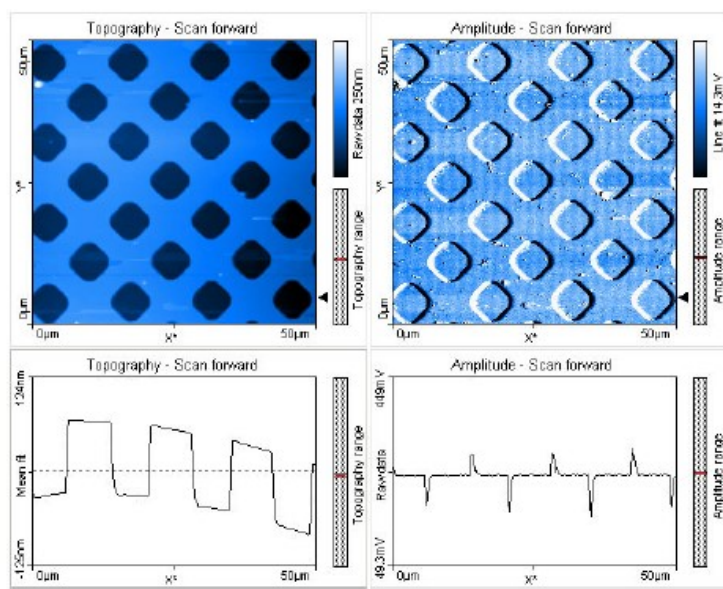


Figure 11 – The 100% ethanol-treated sample of  $C_{60}$

Measurements of the interaction force between fullerene molecules and the substrate carried out in the AFM force spectroscopy mode showed that with increasing ethanol concentration, the bonding force of fullerenes with the substrate decreased significantly. In samples without ethanol, the interaction force was 1.2 nN, indicating that the molecules were strongly bonded to the substrate. However, at 10% ethanol, this force decreased to 1.0 nN, indicating a weakened bond between the fullerene molecules and the substrate surface. The interaction force continued to decrease with increasing ethanol concentration: at 25% ethanol it was 0.8 nN, at 50% it was 0.6 nN, and at 100% ethanol, it was 0.4 nN. These data indicate that with increasing ethanol concentration, fullerenes become less bound to the substrate, which is due to the solvent effect of ethanol and the weakening of the adhesion of fullerenes to the surface.

## 4. Conclusions

The study resulted in several significant conclusions concerning the influence of ethanol on the structure and aggregation properties of C<sub>60</sub> fullerenes, as well as on their interaction with the substrate. When the ethanol-treated C<sub>60</sub> is observed by atomic force microscopy, clear changes in the morphology and nanostructure of the surface are seen, which are attributed to the adsorption of ethanol molecules, the formation of clusters, and the appearance of granularity. These observations are important for further studies of the interaction of fullerenes with various organic solvents and may help in the development of new fullerene-based materials with tailored properties.

One of the key observations was the significant change in the structure of fullerenes as a function of ethanol concentration. In ethanol-free samples, the fullerene molecules formed compact aggregates with a size of about 15-20 nm. However, when ethanol was added, the size of the aggregates began to increase, which is attributed to the solvent effect of ethanol. As the ethanol concentration increased (up to 50-100%), fullerenes formed large and loose aggregates with sizes as large as 80-100 nm. These data indicate that ethanol promotes the dissolution of fullerenes and the increase of intermolecular distances, which leads to the loosening of their structure and an increase in the size of clusters.

In addition, measurements of the interaction force between the fullerene molecules and the substrate showed that the bonding force between the molecules and the substrate decreased significantly with increasing ethanol concentration. At 100% ethanol, the interaction force was the lowest, amounting to only 0.4 nN, which is significantly lower than that of the solvent-free samples, where it was 1.2 nN. This confirms that ethanol weakens the adhesion of fullerenes to the substrate and promotes the separation of molecules from the surface. These changes may be due to the fact that ethanol acts as a solvent, reducing intermolecular interactions and altering the physicochemical properties of fullerenes.

These results confirm the important role of ethanol as a solvent, which not only modifies the structural characteristics of fullerenes but also affects their mechanical properties. Altering the aggregation and interaction of fullerenes with the substrate can be used to develop new nanomaterials as well as technologies where molecular structures and interactions on the surface need to be controlled. In the future, further investigation of the effect of different solvents on fullerenes and their aggregates may open new perspectives in the field of nanotechnology and materials science, allowing the creation of materials with predetermined properties.

## References

- [1] S. V. Lubenets, L. S. Fomenko, V. D. Natsik, and A. V. Rusakova, "Low-temperature mechanical properties of fullerenes: Structure, elasticity, plasticity, strength (Review Article)," *Fiz. Nizk. Temp.*, vol. 45, no. 1, pp. 3–45, Jan. 2019.
- [2] A. Kausar, U. Sheikh, R. Pincak, and M. Pudlak, "Prediction of Buckyballs' physical properties using Sombor index," *Int. J. Geom. Methods Mod. Phys.*, doi: 10.1142/S0219887824502682.
- [3] E. T. Hoke *et al.*, "Recombination in polymer:Fullerene solar cells with open-circuit voltages approaching and exceeding 1.0 V," *Adv. Energy Mater.*, vol. 3, no. 2, pp. 220–230, Feb. 2013, doi: 10.1002/aenm.201200474.
- [4] K. T. Lam, Y. J. Hsiao, L. W. Ji, T. H. Fang, W. S. Shih, and J. N. Lin, "Characteristics of polymer-fullerene solar cells with ZnS nanoparticles," *Int. J. Electrochem. Sci.*, vol. 10, no. 5, pp. 3914–3922, Jan. 2014, doi: 10.1016/s1452-3981(23)06590-2.
- [5] R. Kacimi *et al.*, "Quantum chemical study of symmetrical non-fullerene acceptor chromophores for organic photovoltaics," *Comput. Theor. Chem.*, vol. 1233, p. 114475, Mar. 2024, doi: 10.1016/j.comptc.2024.114475.
- [6] A. Kausar, "Polymer/fullerene nanomaterials in optoelectronic devices: Photovoltaics, light-emitting diodes, and optical sensors," in *Polymer/Fullerene Nanocomposites: Design and Applications*, Elsevier, 2023, pp. 153–174. doi: 10.1016/B978-0-323-99515-3.00006-7.
- [7] S. Thakral and R. Mehta, "Fullerenes: An introduction and overview of their biological properties," *Indian J. Pharm. Sci.*, vol. 68, no. 1, pp. 13–19, Jan. 2006, doi: 10.4103/0250-474X.22957.
- [8] H. J. Johnston, G. R. Hutchison, F. M. Christensen, K. Aschberger, and V. Stone, "The biological mechanisms and physicochemical characteristics responsible for driving fullerene toxicity," *Toxicol. Sci.*, vol. 114, no. 2, pp. 162–182, Nov. 2009, doi: 10.1093/toxsci/kfp265.
- [9] Z. Liu, L. Guo, and J. Zhang, "Application progress of fullerene and its derivatives in medicine," *J. China Pharm.*

- Univ.*, vol. 49, no. 2, pp. 136–146, Apr. 2018, doi: 10.11665/j.issn.1000-5048.20180202.
- [10] S. M. Andreev, E. N. Bashkatova, D. D. Purgina, N. N. Shershakova, and M. R. Haitov, “Fullerenes: Biomedical aspects,” *Immunologiya*, vol. 36, no. 1, pp. 57–61, Jan. 2015.
- [11] B. W. Gao, C. Gao, W. X. Que, and W. Wei, “Recent development of polymer/fullerene photovoltaic cells,” *Wuli Xuebao/Acta Phys. Sin.*, vol. 61, no. 19, p. 194213, Oct. 2012, doi: 10.7498/aps.61.194213.

**Information about authors:**

*Hakhan Ozbay* – PhD, Research Assistant, Department of Physics, Faculty of Science, Erciyes University, Kayseri, Turkey, [hakan.ozbay@tutaimail.com](mailto:hakan.ozbay@tutaimail.com)

**Author Contributions:**

*Hakhan Ozbay* – concept, methodology, resources, data collection, testing, modeling, analysis, visualization, interpretation, drafting, editing, funding acquisition.

**Conflict of Interest:** The authors declare no conflict of interest.

**Use of Artificial Intelligence (AI):** The authors declare that AI was not used.

*Received: 05.11.2024*

*Revised: 10.12.2024*

*Accepted: 20.12.2024*

*Published: 23.12.2024*



**Copyright:** © 2024 by the authors. Licensee Technobius, LLP, Astana, Republic of Kazakhstan. This article is an open-access article distributed under the terms and conditions of the Creative Commons Attribution (CC BY-NC 4.0) license (<https://creativecommons.org/licenses/by-nc/4.0/>).